

Electrical Supplementary Information for

Adhesion and tribological properties of hydrophobin proteins in aqueous lubrication on stainless steel surfaces

Timo J. Hakala^{*a}, Päivi Laaksonen^{ab}, Vesa Saikko^c, Tiina Ahlroos^a, Aino Helle^a, Riitta Mahlberg^a, Hendrik Hähl^b, Karin Jacobs^b, Petri Kuosmanen^c, Markus B. Linder^a and Kenneth Holmberg^a

Wear in pin-on-disc (POD) experiments

Wear of the stainless steel sphere (diameter 10 mm) after sliding on a stainless steel disc was measured from the wear volume of the sphere. Figures S1-S3 present optical microscope images of the wear tracks. The dimensions of the worn area were used for calculation of the wear volume.

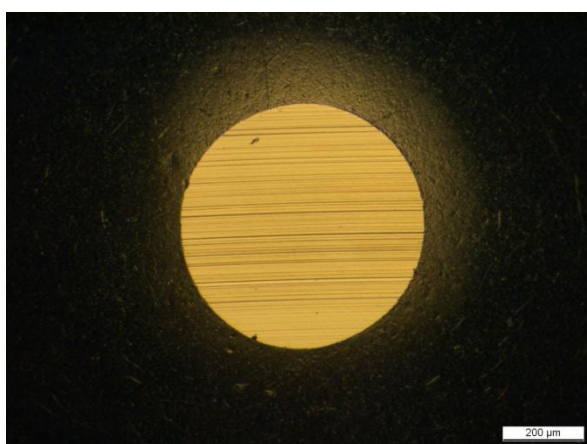


Figure S1. Wear track of the stainless steel sphere after 120 m of sliding on a stainless steel disc. The lubricant was 50 mM sodium acetate buffer pH 5. The scale bar is 200 μm .

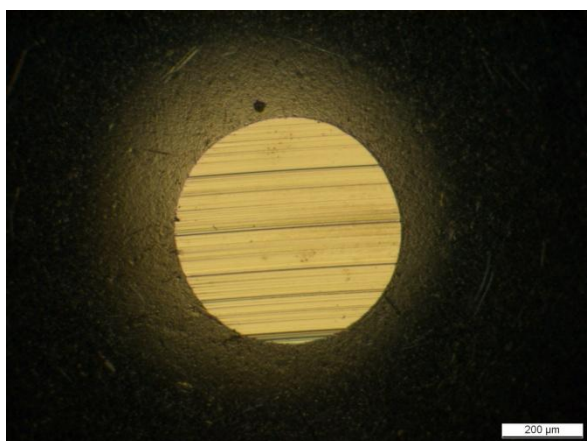


Figure S2. Wear track of the stainless steel sphere after 120 m of sliding on a stainless steel disc. The lubricant was HFBI 1.0 mg/ml in 50 mM sodium acetate buffer pH 5. The scale bar is 200 μm .

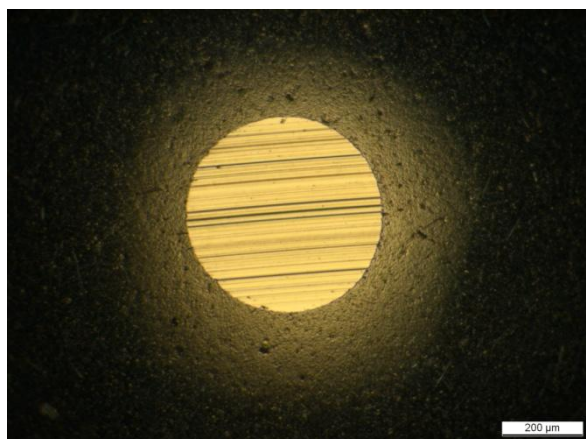


Figure S3. Wear track of the stainless steel sphere after 120 m of sliding on a stainless steel disc. The lubricant was FpHYD5 1.0 mg/ml in 50 mM sodium acetate buffer pH 5. The scale bar is 200 μm .

Transfer in tribological experiments by circular translation pin-on-disc (CTPOD)

In dry sliding, the transfer of polyethylene (UHMWPE) on the stainless steel disc was heavy and the COF was as high as 0.36. Transfer layers were tenacious and could only be removed by repolishing. A microscopy image of the stainless steel surface after a dry experiment is shown in Figure S4.

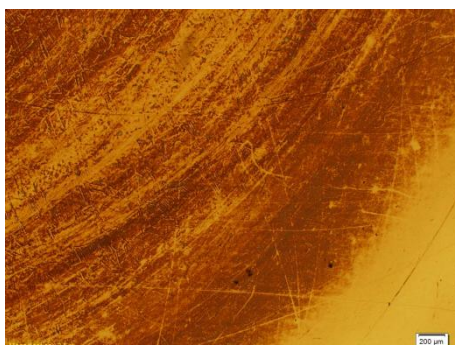


Figure S4. Optical micrograph from the stainless steel disc of a dry test showing the UHMWPE transfer layer. Edge of contact zone. Lower right corner shows original polished surface. The scale bar is 200 μm .

FTIR was used to investigate the polyethylene transfer on the stainless steel disc (Fig. S5). It was observed that hydrophobins were able to reduce transfer compared to plain buffer solution.

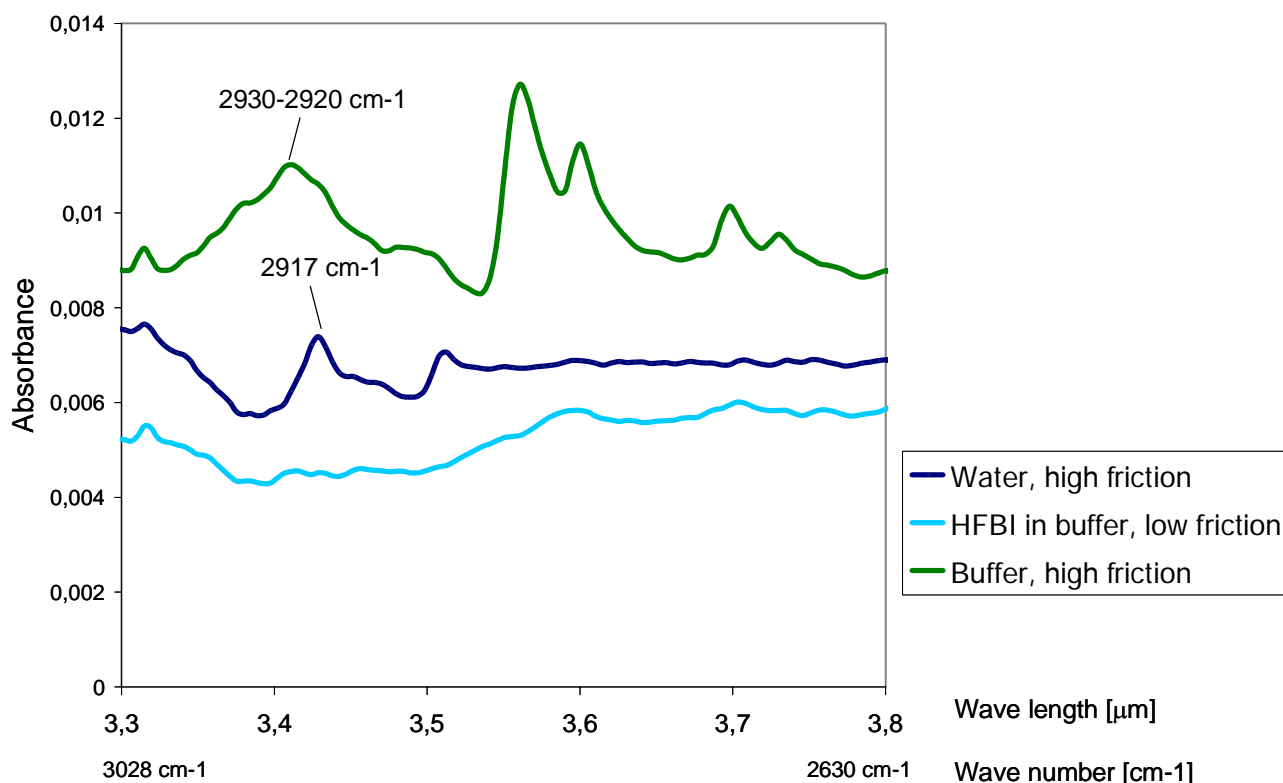


Figure S5. FTIR spectra (from top to bottom) of the CTPOD discs lubricated 1) with the sodium acetate buffer (high COF values), 2) with water (high COF values) and 3) with the 0.1 mg/ml HFBI in the buffer (low COF values). The absorbance bands at 2917-30 cm^{-1} are due to asymmetric CH_2 stretching and at 2849-50 cm^{-1} due to symmetric CH_2 stretching of polyethylene. Residues of the solid buffer were obtained on the disc lubricated with the buffer (additional absorption bands are seen in the top spectrum).

Marked deformation of the wear surface of the pin was common when UHMWPE vs. stainless steel contact was lubricated by the 50 mM sodium acetate buffer (Fig. S6).

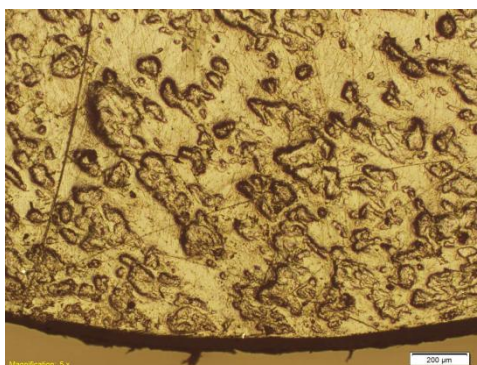


Figure S6. Optical micrograph from the edge of the UHMWPE pin worn in the sodium acetate buffer, showing typical protuberance formation caused by multidirectional motion, creep deformation, and possibly some thermal phenomena. The scale bar is 200 μm .

Friction in tribological experiments by circular translation pin-on-disc (CTPOD)

In UHMWPE vs. stainless steel contact the hydrophobins were not reducing the coefficient of friction compared to 50 mM sodium acetate buffer.

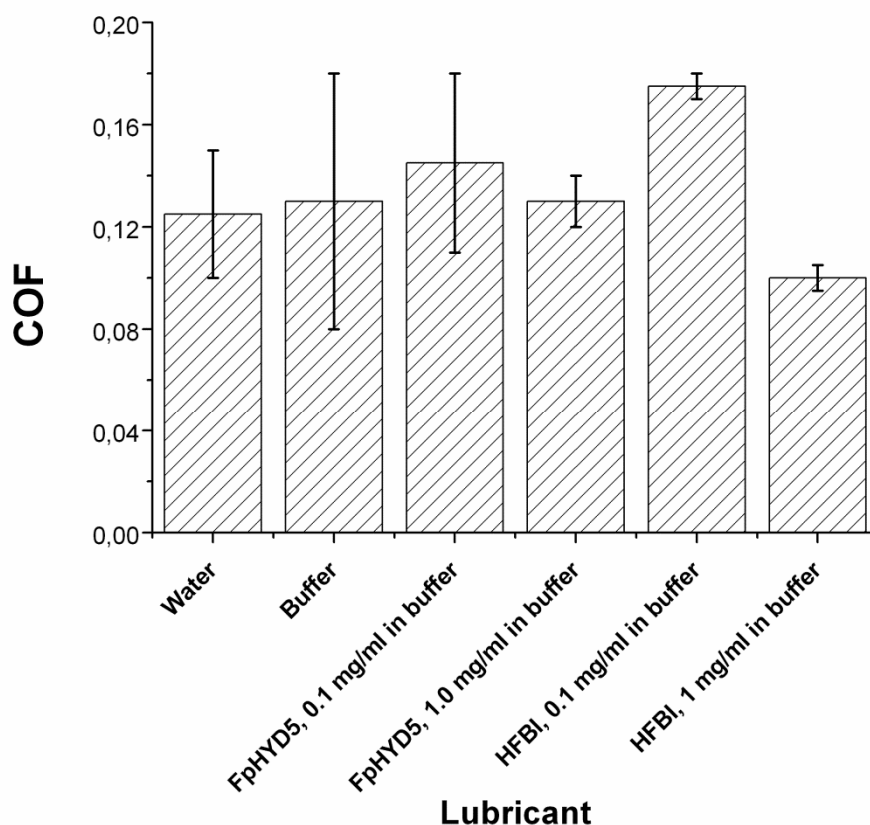


Figure S7. Coefficients of friction in lubricated UHMWPE vs. stainless steel contact. The buffer was 50 mM sodium acetate buffer pH 5. the coefficient of friction is presented as the average value of minimum and maximum. Scatter is presented as minimum and maximum.

Dynamics of protein adsorption on stainless steel

The dynamics of the protein adsorption was studied by analysing the binding of the proteins as a function of time. The binding curves measured by QCM are shown in Figure S8 and those measured by ellipsometry are shown in Figure S9. A simple Langmuir-type adsorption curve was fitted to the curves in order to extract a rate constant for the binding.

$$m_{\text{ads}} = B_{\text{max}}(1 - e^{-kt}) \quad (\text{Eq. S1})$$

Here B_{max} is the amount of bound protein in equilibrium and k is the rate constant of binding. The resulting rate constants as a function of concentration are presented in Figure S10. HFBI showed a more pronounced dependence on the protein concentration.

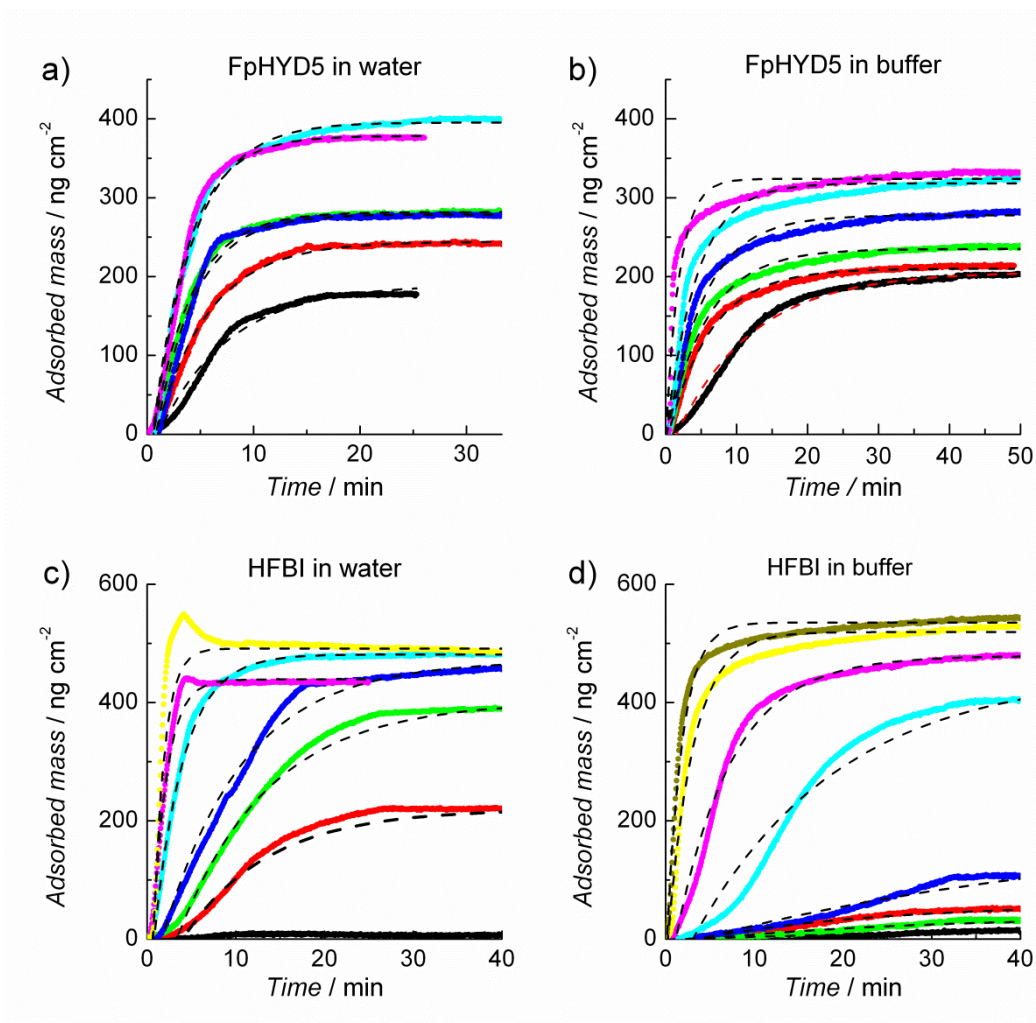


Figure S8: Adsorbed mass of FpHYD5 (a,b) and HFBI (c,d) on steel measured by QCM-D. Adsorption of FpHYD5 was measured in water (a) and in 50 mM NaAc buffer (b) at concentrations 0.1 (purple), 0.05 (cyan), 0.025 (blue), 0.01 (green), 0.005 (red) and 0.0025 g L⁻¹ (black). Adsorption of HFBI was measured in water (c) at concentrations 0.25 (yellow), 0.1 (purple), 0.05 (cyan), 0.025 (blue), 0.01 (green), 0.005 (red) and 0.0025 L⁻¹ (black) and in 50 mM NaAc buffer (d) at concentrations 0.25 (olive), 0.1 (yellow), 0.05 (purple), 0.025 (cyan), 0.01 (blue), 0.0075 (green), 0.005 (red) and 0.0025 g L⁻¹ (black). The dashed curves show the curves fitted to the measured data.

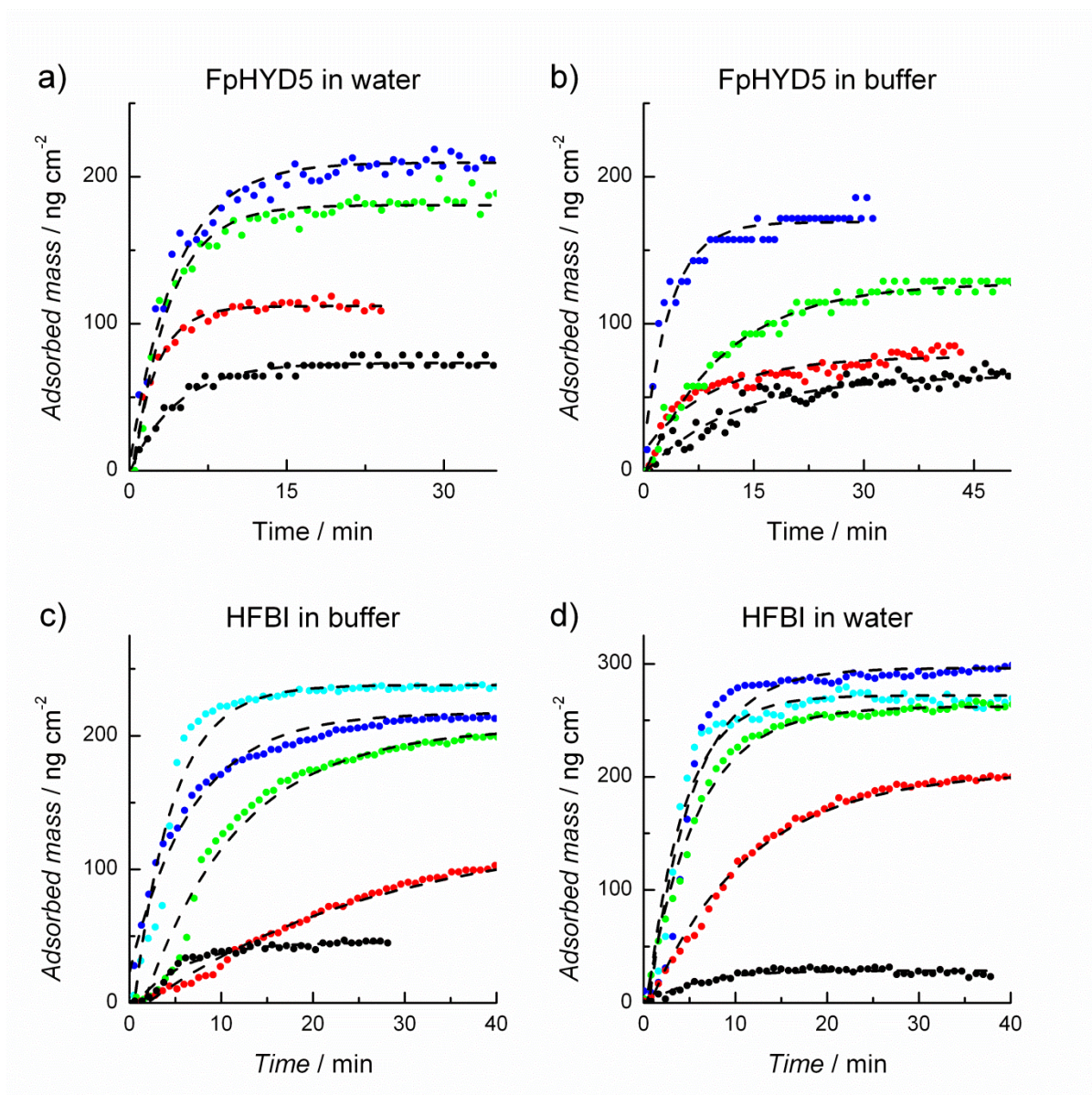


Figure S9. Adsorbed mass of FpHYD5 (a,b) and HFBI (c,d) on steel measured by ellipsometry. Adsorption of FpHYD5 was measured in water (a) and in 50 mM NaAc buffer (b) at concentrations 0.1 (blue), 0.025 (green), 0.0125 (red), 0.005 g L⁻¹ (black). Adsorption of HFBI was measured in water (c) and in 50 mM NaAc buffer (d) at concentrations 0.1 (cyan), 0.05 (blue), 0.025 (green), 0.0125 (red) and 0.005 g L⁻¹(black). The dashed curves show the curves fitted to the measured data.

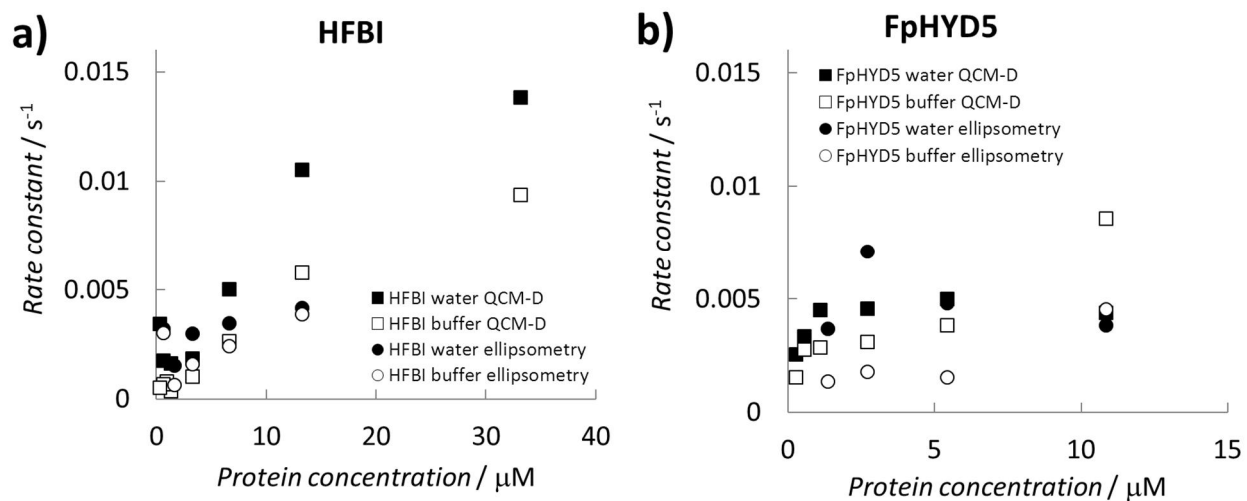


Figure S10. Rate constants extracted from the exponential decay fits.